

Research article

Self-healing behaviour of lignin-containing epoxidized natural rubber compounds

Bedriye Nur Yeşil¹, Tuba Ünügül¹, Bağdagül Karaağaç^{1,2*}

¹Department of Chemical Engineering, Kocaeli University, Umuttepe Campus, 41380 Kocaeli, Turkey

²Department of Polymer Science & Technology, Kocaeli University, Umuttepe Campus, 41380 Kocaeli, Turkey

Received 10 November 2022; accepted in revised form 21 February 2023

Abstract. Epoxidized natural rubber (ENR) is a relatively new raw material that can be used in many applications, such as rubber-based adhesives, self-crosslinking, and compatibilization of rubber and filler matrices in favor of reactive epoxy groups. However, as almost all types of polymeric materials do, ENR is exposed to mechanical, chemical, and thermo-oxidative degradation during service life, resulting in micro- and macro-cracks in the material body as well as on the surface. The self-healing approach is considered a good solution to provide longer service life by instantaneous repairing these cracks by means of internal and external stimulants. In literature, most attempts at self-healing of ENR focus on irreversible covalent bond based systems. In this study, lignin and a common anti-reversion agent 1,3-bis(citraconimido-methyl) benzene (CIMB) have been evaluated for carrying out self-healing through reversible covalent bonds via Diels-Alder interaction between ENR and CIMB. In addition, lignin could significantly improve self-healing by promoting an epoxy ring-opening reaction on the ENR backbone. The best healing conditions were selected as 180 °C and 15 minutes, and 83% self-healing was achieved by incorporating 6 phr lignin and 15 phr CIMB into the reference compound. Satisfactory self-healing performance has been attributed to the synergistic effect of lignin and CIMB.

Keywords: material testing, lignin, mechanical properties, rubber, self-healing

1. Introduction

Because of irreversible cross-links, rubber-based materials may undergo a structural deformation at either the micro- or the macro-level when exposed to external effects such as chemical, radiative, oxidative, and/or UV-based effects. Since those deformations or fractures continue to build up during the service life of rubber material, its performance gradually decreases over time. It is crucial in most applications not only to avoid the visible effects of those deformations over the material, at least temporarily during the material's service life, but also to ensure a long-lasting performance to be similar or comparable to its initial value. Thus, the 'self-healing' approach for rubber materials has been studied extensively for the last couple of years [1–3]. Self-healing

is the ability of a material to repair the micro- and macro-failures in its structure with or without the help of an external stimulant. External and internal self-healing are the two main approaches suggested [4, 5]. The external self-healing approach suggests self-healing by using healing agents. The internal self-healing approach, on the other hand, suggests a healing process without the need for healing agents, instead depends on the functional groups on the chemical structure of the material and their ability to create reversible non-covalent interactions such as H-bonds, metallic interactions as well as metal-ligand interactions [6–8].

Epoxidized natural rubber (ENR) is synthesized by chemically controlled modification of the natural rubber (NR) with formic peroxy acid. This novel raw

*Corresponding author, e-mail: bkaraagac@kocaeli.edu.tr

© BME-PT

material is commercially available depending on its molar epoxy content. Thanks to its rigidity, ENR is widely used in the automotive and aviation industries for the manufacture of joints, bumpers, gaskets, sealants, sponges, cross-linked pipes, and pressure-sensitive adhesives. It is also used for the manufacture of medical tapes, plasters, and carpet backings [1, 9–11]. In the presence of reactive epoxy groups, ENR can further be used in self-crosslinking applications as a compatibilizer for polar fillers and as an adhesion enhancer between rubber and metal structures [12–15]. In addition to the above, ENR can undergo a dual cross-linking process via its C=C double bonds and reactive epoxy sites. Sulfur cross-linking can occur over allylic H atom on C=C double bond, whereas secondary cross-links are initiated by the essential compound additives containing amino, chlorine, and carboxyl functional groups as a result of epoxy chain opening reaction [16–18].

The existence of reactive epoxy groups on ENR may lead to the regeneration of already broken polymer chains where appropriate conditions exist. There are a few studies met in the literature on the self-healing of ENR [7, 19–22]. Imbernon *et al.* [19] investigated the self-healing behavior of ENR-based rubber compounds containing dithiobutyric acid with reactive disulfide groups (DTDB). In this study, they reported ENR to exhibit standard natural rubber characteristics up to 100 °C, whereas self-healing could occur as a result of cross-linking disulfide groups after rearrangement between polymer chains above 150 °C. In another study, Xu *et al.* [21] investigated the self-healing mechanism of carboxymethyl chitosan incorporated ENR latex, where they achieved 90% self-healing by means of reversible H-bonds between ENR and carboxymethyl chitosan molecules. Liu *et al.* [20] investigated the self-healing characteristics of two different types of zinc methyl acrylate incorporated ENR (ENR-25 and ENR-40) at various time and temperature conditions, where they considered the tensile properties as the criteria for success. They achieved 80% self-healing for ENR-40 conditioned at 80 °C for 1 h and 70% for ENR-25 conditioned at 30 °C for 50 min. Self-healing by Diels-Alder reaction is an easier and much more practical method than the other self-healing methods as it can be performed by using solely heat rather than using a catalyst or pre-treatment on the monomer or fractured surface [23, 24]. Self-healing of cross-linked materials can be achieved as a result of the formation of

the thermally reversible covalent bonds in the Diels-Alder mechanism. In self-healing applications of rubber, which are assisted by the Diels-Alder mechanism, materials containing highly electronegative and reactive furan/maleimide groups are used for the formation of a dien-dienophyl couple [25–27]. Bismaleimides are reactive products where maleimide units exist on dianhydride or diamine terminal groups. The carbonyl groups linked to the terminal site of maleimides act as dienophiles in order to undergo a Diels-Alder reaction with the double bond conjugated dienes of bismaleimides. In rubber technology, bismaleimides are mainly as co-agents in peroxide vulcanization and anti-reversion agent in sulfur vulcanization of highly unsaturated rubbers [28, 29]. 1,3-bis(citraconimidomethyl)benzene (CIMB) is used as an anti-reversion agent used in sulfur vulcanization, and it acts by altering the reaction mechanism to avoid reversion. CIMB can undergo cyclo-addition reactions by the Diels-Alder mechanism to recombine diene and triene structures which formed as a result of chain scission due to various deteriorating external factors [30]. In this study, unlike its accustomed use, the use of CIMB in the Diels-Alders addition reaction was investigated to identify its effect on the self-healing process over the rubber materials.

Lignin is a worldwide available biopolymer that can be extracted from plant cell walls. More than 50 million tonnes of lignin is produced as a by-product of craft and bio-ethanol manufacturing processes. Lignin, an amorphous biopolymer, exhibits various properties depending on its monomeric composition and substituents. This monomer has reactive functional groups such as aliphatic hydroxy, phenolic hydroxy, methoxy, carbonyl, and carboxyl, allowing the preparation of graft copolymers with a wide range of industrial chemicals [31–38]. The reactivity of lignin mainly depends on its functional groups as well as molecular weight distribution and solubility properties [39–42]. Lignin is an abundant and low-cost additive that provides stability and good mechanical properties to the compositions thanks to the presence of aromatic structures. It can undergo a broad range of chemical transformations and provide hydrophilic or hydrophobic characteristics depending on its origin. Furthermore, lignin can be used to protect the materials against oxidative degradations, and it is more resistant to most biological attacks than cellulose and other structural polysaccharides [39, 43, 44]. The chemical functionalities in lignin are

able to react with the epoxy sites of ENR, making lignin the cross-linking center of the lignin/ENR composites [45]. –OH functionality, which induces self-healing via the formation of hydrogen bonding with ENR [4].

Lignin is categorized into two major methods of isolation: sulfur and sulfur-free lignin extraction processes. Sulfur lignin comprises kraft lignin and lignosulphonate lignin, which are primarily produced by paper and pulp industries. Kraft lignin is hydrophobic and contains a high level of condensed structures, phenolic hydroxyl groups, and aliphatic thiol groups [46–48]. Lignosulphonates are water soluble, contain sulfur in the form of sulfonate groups present on their aliphatic side chains, and are produced of waste liquid from softwood [49]. They have a higher average molar mass than kraft lignin with a broad polydispersity [49, 50]. Sulfur-free lignin generally is a low molecular weight product of high purity.

In recent years, many studies related to the use of lignin in rubber compound formulations have been reported. Most of those studies have focused on the use of lignin as a reinforcing filler, anti-aging agent, adhesion enhancer, and additive to improve the thermal and mechanical properties of rubber compounds [38, 43, 45, 51]. Some other studies focused on cross-linking reactions in the presence of lignin. Jiang *et al.* [45] investigated lignosulphonate lignin (0–40 phr)/ENR blends, which were prepared at 180 °C and in the absence of traditional rubber cross-linking agents such as sulfur and peroxide. They measured cross-linking degree, glass transition temperature, mechanical and dynamic-mechanical properties. The results showed lignin to provide higher cross-link density by inducing the epoxy ring-opening reaction of ENR. However, a relatively higher amount of lignin caused poor rubber-filler interaction and lower tensile modulus due to insufficient compound homogeneity. Besides, lignin may undergo a Diels-Alders cyclo-addition reaction if already functionalized with furan and/or maleic anhydride groups incorporated furan functionality to lignin by the reaction between furfuryl glycidyl ether and phenolic OH groups of lignin [52]. Lignin's phenolic and aliphatic groups have also reacted with maleimidohexonic acid to provide maleimide groups onto lignin. These functionalized lignins were then combined to form a gel structure via a Diels-Alder reaction at 70 °C. The gel structure could be reversed into a liquid state at 120 °C, where the reaction was called retro-Diels-Alder.

Despite several studies about both self-healing of rubber compounds and cross-linking rubber by means of lignin, there is not any study met in the literature on the self-healing of lignin-containing regular rubber compounds. In this study, the self-healing behavior of ENR-based rubber compounds in the presence of lignin and CIMB has been investigated. The rheological and mechanical properties of the rubber compounds were also measured. The effects of varying time and temperature on self-healing performance have been evaluated.

2. Experimental

2.1. Materials

ENR-50 (Epoxyrene), which has 50% (mol%) epoxy content and 80±5 MU Mooney viscosity, was purchased from Muang Mai Guthrie Public Company Ltd. (Thailand). Lignin alkali with 5% humidity and 6.5 of pH value was obtained from Sigma Aldrich. 1,3-bis(citraconimidomethyl)benzene was purchased from Lanxess Deutschland GmbH (Germany) with the commercial name of Perkalink 900. HAF N330 carbon black (CB, filler) was originated from OMSK (Russia). Zinc oxide (activator, White Seal, 325 mesh particle size) was rubber grade and purchased from Metal Oksit (Turkey). Stearic acid (activator, 52–62 °C of congealing point) was also standard rubber grade additive and was purchased from Zeta Kauçuk (Turkey). Antioxidants; polymerized 2,2,4-trimethyl-1,2-dihydroquinoline (TMQ), *N*-isopropyl-*N'*-phenyl-*p*-phenylenediamine (IPPD), and ozone wax were obtained from Zeta Kauçuk (Turkey). TMQ, with a softening point of 90 ±10 °C, whereas IPPD was of 70 °C. Curing system components; *N*-cyclohexyl-2-benzothiazole sulfenamide (CBS, accelerator) and insoluble sulfur (vulcanization agent, 80% purity), both contained 80% active substance and 20% elastomer binder; they were purchased from Zeta Kauçuk (Turkey). All additives were commercially available and used as received.

2.2. Preparation of compounds and test procedures

Rubber compounds were prepared by using a 2 l (gross volume) internal mixer (Met-Gur, Turkey) and sheeted out on a laboratory mill subsequently. Firstly, epoxidized natural rubber was masticated for 2 min at a rotor speed of 30 rpm to obtain desired flow properties. Carbon black, lignin, and process oil were then fed into the mixer and mixed for 1 min

at 25 rpm. The rotor speed was kept constant at 25 rpm during the rest of the mixing. In the next three steps, a 30 s interval was applied between activators (zinc oxide and stearic acid), stabilizers (TMQ, IPPD, and ozone wax), and the curing system, including CIMB (CBS, sulfur, and CIMB). The final compound was then mixed 1 min further and dumped from the mixer at approximately 60 °C. A 150 mm wide laboratory-type two-roll mill with a friction ratio of 1:1.1 was used for the final homogenization and shaping of the compound. 5 cycles of wound-up with a 3 mm nip thickness were performed on the mill to ensure a standard mixing process.

Compound formulations are given in Table 1. In Group 1, REF is the control compound, which does not comprise any of lignin and CIMB as the self-healing agent. LA3 and LA6 comprise 3 and 6 phr lignin alkali, respectively. Compounds comprising only CIMB are in Group 2, and various amounts of CIMB were used in these compounds. Group 3 and Group 4 comprise both agents in various amounts, where the amounts are also indicated by the compound codes.

Alpha Pioneer 2000 model moving die rheometer (MDR) was used to measure the optimum cure times of the rubber compounds according to ASTM D5289. Minimum torque (M_L), maximum torque (M_H), scorch time (t_{s2}), and optimum cure time (t_{90}) were measured; cure extent (CE) and cure rate index (CRI) parameters were calculated according to the

standard. Compounds were vulcanized on a hydraulic hot press under 150 bar pressure and for their respective optimum cure times (time corresponding to maximum torque) at 150 °C. Test samples were then cut from the vulcanized sheets by using standard sharp blades.

Mechanical properties of Die C dumb-bell shaped vulcanizates were measured by using a universal testing machine (Instron 3345) with 500 mm/min crosshead speed according to ASTM D412. Tensile strength, elongation at break, and tensile stress at 50% elongation (50% modulus) values were recorded. 5 samples for each compound were tested, and the average value was reported as a result.

A self-healing study was performed on tensile-fractured samples, which were manually re-attached to establish contact between two fractured surfaces in an ASTM D412 Die C-sized mold at selected healing temperatures (160, 170, 180 and 190 °C) for 5, 10 and 15 minutes in the air over operating at ambient pressure. The minimum healing temperature was selected as 160 °C after prior analysis for obtaining meaningful self-healing performance. After healing at the specified conditions, the self-healed specimens were subjected to tensile testing. 5 samples were tested and the average value was used to calculate and report the self-healing ratio. The self-healing performance of the samples was evaluated by means of their percentage retention in tensile strength values as well as by their visual inspection. Equation (1)

Table 1. Rubber compound formulations.

	Group 1			Group 2			Group 3			Group 4		
	REF	LA3	LA6	4 CIMB	10 CIMB	15 CIMB	LA3-4 CIMB	LA3-10 CIMB	LA3-15 CIMB	LA6-4 CIMB	LA6-10 CIMB	LA6-15 CIMB
	Content [phr]											
ENR	100	100	100	100	100	100	100	100	100	100	100	100
CB (N-330)	40	40	40	40	40	40	40	40	40	40	40	40
Lignin	–	3	6	–	–	–	3	3	3	6	6	6
CIMB	–	–	–	4	10	15	4	10	15	4	10	15
Process oil	10	10	10	10	10	10	10	10	10	10	10	10
Zinc oxide	5	5	5	5	5	5	5	5	5	5	5	5
Stearic acid	2	2	2	2	2	2	2	2	2	2	2	2
TMQ	2	2	2	2	2	2	2	2	2	2	2	2
IPPD	1	1	1	1	1	1	1	1	1	1	1	1
Ozone wax	2	2	2	2	2	2	2	2	2	2	2	2
CBS	2	2	2	2	2	2	2	2	2	2	2	2
Sulfur	2	2	2	2	2	2	2	2	2	2	2	2

was used to calculate self-healing performance, where σ_i represents the original mechanical property (tensile strength) of the sample, and σ_f is the value of the same property of the same sample after self-healing [53, 54]. Visual inspection of healed samples was performed by using a MicroDirect 1080p HD (Celestron LLC, USA) microscope (Equation (1)):

$$\text{Self-healing ratio [\%]} = \frac{\sigma_f}{\sigma_i} \cdot 100 \quad (1)$$

The swelling ratio of the samples was measured according to ASTM D471-12. For each compound, 5 samples were taken from healing surfaces, they were first subjected to ambient acetone extraction for 24 h, and dried in an air oven for a further 24 h prior to measuring initial weight is recorded as W_s . Each sample was immersed in toluene at ambient temperature for 72 h and dried in an air oven for 24 h until a constant mass (final weight, W_{ds}) could be obtained. Swelling ratio (Q), cross-link density (V_e), and the molecular weight between the cross-links (M_c) were calculated by using Equation (2), Equation (3), and Equation (4), respectively according to Flory-Rehner approach [26, 55, 56]:

$$Q = \frac{W_s}{W_{ds}} - 1 \quad (2)$$

$$V_e = \frac{-[\ln(1 - V_2) + V_2 + \chi V_2^2]}{V_s(V_2^{1/3} - \frac{V_2}{2})} \quad (3)$$

$$V_e = \frac{1}{2M_c} \quad (4)$$

where W_s and W_{ds} are the weight fraction of the polymer respectively in swollen and de-swollen phases, V_2 is the volume fraction of the rubber in swollen phase, V_s is the molar volume of the solvent, which is 106.3 ml/mol for toluene, and χ is the solvent-rubber interaction parameter. χ was taken as 0.34 for the toluene-ENR system [57, 58].

A Fourier transform infrared spectrometer (FTIR, Perkin Elmer Spectrum 100, PerkinElmer Inc., USA) was used to investigate structural analysis. The selected spectral resolution and the scanning range were installed as 4 scans and from 650 to 4000 cm^{-1} , respectively.

Dynamic mechanical analyzer (DMA, DMA 50, Metravid Design, France) was used for measuring both storage and loss moduli of the samples for 40–180 °C temperature range at 1 Hz frequency and 0.1% strain

amplitude conditions to investigate Diels-Alder and retro-Diels-Alder reactions during the self-healing process. Samples were subjected to three temperature cycles. In each cycle, samples were first heated to 180 °C by 10 °C/min, held at 180 °C for 15 minutes, and then cooled down to 40 °C by 2 °C/min cooling rate. Here, 180 °C and 15 min parameters were used for representing the optimum self-healing conditions, which were mentioned in the following parts of the paper.

3. Results and discussions

3.1. Rheological properties

Rheometer curves of four compound groups were obtained at 150 °C, and they are all shown in Figure 1. Common rheological parameters are also given in Table 2. Cure extent (CE) values were calculated as the difference between the maximum and minimum torque values (M_H and M_L) in dNm. Cure rate index [min^{-1}] of the rubber compounds was calculated using Equation (5) [59, 60].

$$CRI = \frac{100}{t_{90} - t_{s2}} \quad (5)$$

As seen from Figure 1 and Table 2, incorporating CIMB into the REF compound along with lignin resulted in a 35–40% lower M_L value. It is more pronounced in the case of high CIMB levels and attributed to the plasticizing effect of CIMB as a processing aid [61]. For Group 1 compounds in Figure 1a, a relatively higher amount (6 phr) of lignin could considerably improve the maximum torque value. In contrast to lignin, the incorporation of CIMB did not lead to an increase in M_H , and lower M_H values also were obtained with increasing CIMB content for Group 2 (Figure 1b) compounds. Anti-reversion effect of CIMB was obvious for all the compounds comprising CIMB, as expected [62, 63]. For Group 3 (Figure 1c) and Group 4 (Figure 1d) compounds, which contain both lignin and CIMB, overall curing characteristics were measured as between those of Group 1 and Group 2 compounds. A remarkable increase (up to 40%) was noticed in the cure rate index for the compounds that comprise both lignin and CIMB when compared to the reference compound. This finding is attributed to reactive functional groups of lignin and CIMB to promote the epoxy ring-opening reaction on the ENR matrix and so to ensure further cross-linking reactions [45, 64, 65].

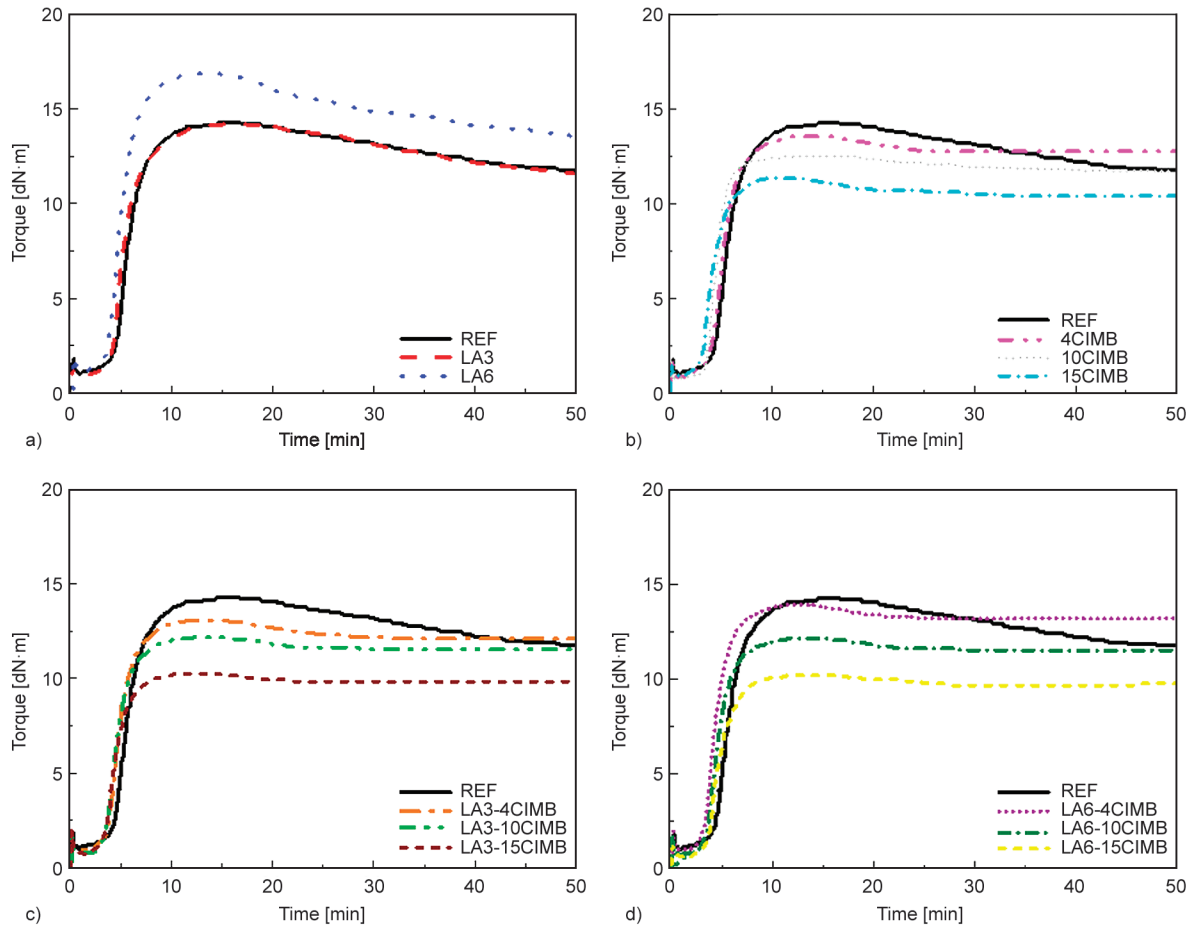


Figure 1. Rheometer curves obtained at 150 °C of a) Group 1, b) Group 2, c) Group 3 and d) Group 4.

Table 2. Rheological properties.

	M_L [dN·m]	M_H [dN·m]	t_{s2} [min]	t_{90} [min]	CE [dN·m]	CRI [min ⁻¹]
REF	1.1	14.5	4.51	8.36	13.4	26.0
LA3	0.9	14.2	4.22	8.52	13.3	23.3
LA6	1.0	16.7	3.53	7.11	15.8	27.9
4CIMB	0.9	13.5	4.15	7.43	12.6	30.5
10CIMB	0.8	12.5	3.93	6.91	11.7	33.6
15CIMB	0.7	11.6	3.50	6.31	10.8	35.6
LA3-4CIMB	0.9	13.1	3.91	7.09	12.1	31.5
LA3-10CIMB	0.7	12.1	3.70	6.83	11.4	32.0
LA3-15CIMB	0.7	10.4	3.67	6.53	9.7	35.0
LA6-4CIMB	0.9	14.0	3.38	6.95	13.1	28.0
LA6-10CIMB	1.2	11.7	3.51	6.64	10.5	32.0
LA6-15CIMB	0.6	9.7	3.32	6.04	9.0	36.8

3.2. Tensile properties

The tensile test results of the original samples are given in Table 3. Although any enhancement in the mechanical performance of the REF compound was expected in this study, it would be helpful to figure out the overall effects of lignin and CIMB on ENR. It is seen from the table that both lignin and CIMB adversely affected the mechanical strength. However,

most of the compositions still have acceptable material properties, and they can also be improved by various methods when the original material properties are of interest.

As can be clearly seen from Table 3, both additives resulted in lower tensile strength, elongation at break, and 50% modulus values. Indeed, blending lignin with most polymers is not straightforward because

Table 3. Original mechanical properties of the vulcanizates.

	Tensile strength [MPa]	Elongation at break [%]	50% Modulus [MPa]
REF	16.4±1.4	889±60	0.96±0.05
Group 1			
LA3	14.0±1.0	835±43	0.84±0.04
LA6	13.4±1.9	643±58	1.20±0.06
Group 2			
4CIMB	11.8±1.0	797±45	0.81±0.02
10CIMB	10.5±1.0	716±53	1.14±0.05
15CIMB	10.5±0.3	687±29	0.99±0.03
Group 3			
LA3-4CIMB	14.2±1.4	895±80	0.85±0.02
LA3-10CIMB	13.6±1.3	760±53	0.74±0.03
LA3-15CIMB	10.5±0.7	624±58	0.75±0.09
Group 4			
LA6-4CIMB	14.5±0.8	658±25	1.05±0.03
LA6-10CIMB	13.7±0.8	642±39	0.92±0.03
LA6-15CIMB	7.5±0.8	525±80	0.69±0.08

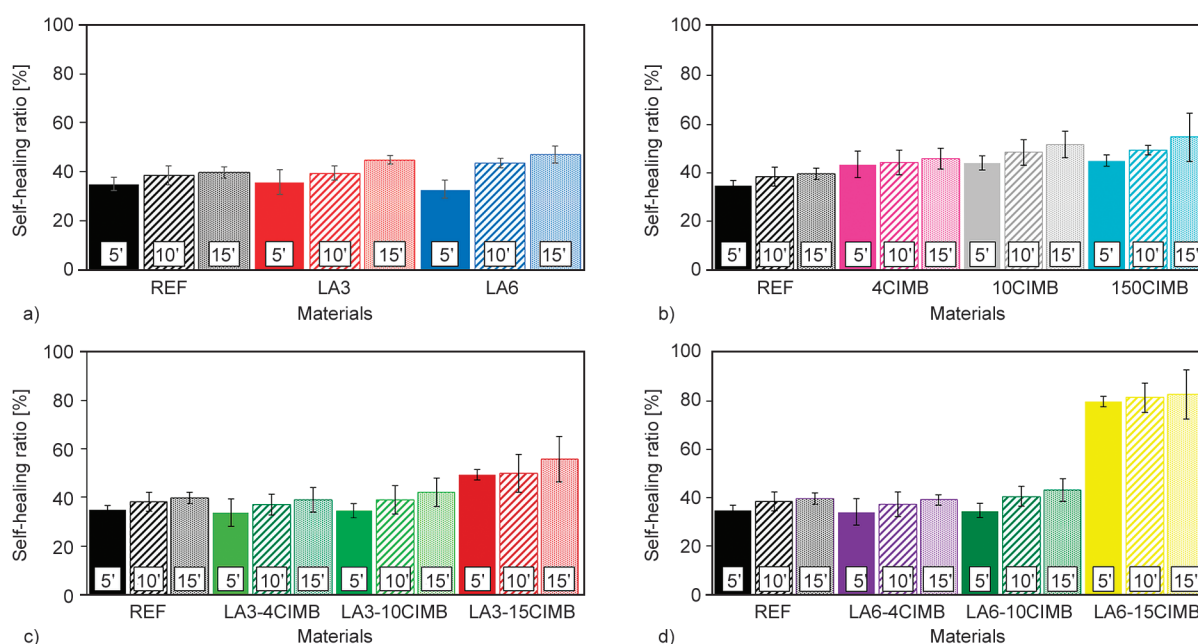
of its polar character and may result in a poor matrix interface [66]. CIMB has been found to have a higher impact on tensile properties compared to lignin due to its plasticizing effect [51]. However, particularly at lower (4 and 10 phr) CIMB levels, the presence of lignin could dampen the deteriorative effect of CIMB. Interactions between lignin and CIMB are most probably due to phenolic hydroxyl groups of lignin. The phenolic hydroxyl groups are the most reactive functional groups and can significantly affect the chemical reactivity of the material [43, 47, 67].

3.3. Self-healing study

Along with their visual inspection, the self-healing performance of the samples was evaluated by means of their retention in tensile strength values. Self-healing performance results at 180 °C and for 5, 10, and 15 min healing times are given for four different compound groups, separately in Figure 2.

It is seen in Figure 2 that ENR-based control compound (REF) exhibits 27–38% healing at elevated temperatures on its own. This was already an expected result due to the well-known limited self-cross-linking ability of ENR [14, 45]. As seen in Figure 2a, 3 phr lignin incorporation did not improve the self-healing performance of the reference compound except at relatively high healing temperatures. However, up to 47% healing could be obtained for the LA6 compound when sufficient healing time was allowed. Here, another interesting finding is that the maximum self-healing ratio for all compounds was measured at 15 min healing time. Although there is no proven temperature limit, lower self-healing performance at 190 °C has been attributed to competitive reactions in rubber matrix, in which one was healing, and the other one was chain scission resulting in lower tensile strength after self-healing.

As one can see in Figure 2b (Group 2), CIMB could improve self-healing performance from 27–38 to 35–55%. 55% self-healing ratio was measured for 15CIMB compound at 180 °C for 15 min healing time. However, it should be noted that there was

**Figure 2.** Self-healing ratio for various healing times at 180 °C; a) Group 1, b) Group 2, c) Group 3 and d) Group 4.

not a remarkable change in average self-healing performance when the amount of CIMB was increased from 10 to 15 phr in the compound.

Self-healing performance was also evaluated for the longest healing time (15 min), and the effect of healing temperature at 160, 170, 180, and 190 °C is shown in Figure 3. Contrary to Group 1 compounds, increasing the healing temperature of the 15CIMB compound did not cause a deterioration in self-healing performance. This was solely attributed to the anti-reversion effect of CIMB, which is also more pronounced at high temperatures.

Group 3 compounds comprise 3 phr lignin and CIMB ladder (Table 4). Here, any of the compounds did not exhibit an improvement in self-healing ratio when compared to Group 2 compounds, which comprise only CIMB in the same amounts as Group 3. The highest self-healing ratio for Group 3 was measured as 55%; this was of the LA3-15CIMB compound and measured at 180 °C – 15 min healing conditions (Figure 2d). When we compare Group 1 and Group 2 in each other, CIMB is still found to improve healing by balancing self-healing and reversion processes.

Using a relatively high amount (6 phr) of lignin with an increasing amount of CIMB (Group 4) was evaluated in Figure 2 and Figure 3. As seen in both figures, when the healing temperature was increased sufficiently, 6 phr lignin and 15 phr CIMB (LA6-15CIMB) could provide remarkable success in self-healing. This was also related to healing time. The

Table 4. Self-healing ratio [%] in tensile strength of the vulcanizates for 15 min.

	at 160 °C	at 170 °C	at 180 °C	at 190 °C
REF	32±1	33±3	40±2	37±3
Group 1				
LA3	30±3	34±5	45±2	34±8
LA6	31±4	36±3	47±3	43±8
Group 2				
4CIMB	35±3	40±1	46±4	50±5
10CIMB	42±4	44±8	52±5	55±5
15CIMB	43±7	44±7	55±10	55±5
Group 3				
LA3-4CIMB	27±3	36±3	39±5	38±5
LA3-10CIMB	33±6	38±5	42±6	41±5
LA3-15CIMB	44±3	45±4	56±9	48±9
Group 4				
LA6-4CIMB	27±3	36±5	39±2	41±1
LA6-10CIMB	34±3	39±4	43±4	42±4
LA6-15CIMB	58±3	63±11	83±10	78±8

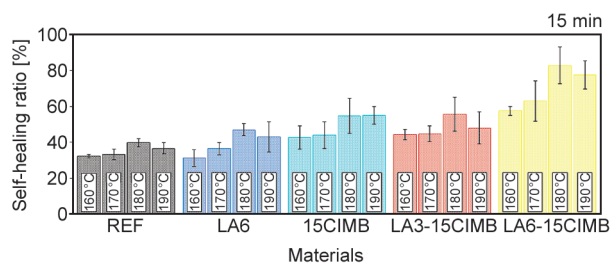


Figure 3. Self-healing ratio at various temperatures for 15 minutes healing time.

highest level of self-healing, which was 83%, again could be obtained at 180 °C. This impressive healing ratio was attributed to the best stoichiometric interaction between lignin and CIMB.

Structural mobility and localization are the key concepts for self-healing. Thus, high cross-link density is expected to reduce self-healing due to the fact that it restricts mobility in the polymeric matrix [68]. Indeed, there are some studies met in the literature indicating reciprocity between self-healing and cross-link density for ENR-based rubber compounds [1, 17, 69, 70] as well as for different polymeric structures [6, 71, 72]. In this study, the LA6-15CIMB compound exhibits not only the highest level of self-healing performance but also the lowest level of tensile modulus along with the lowest cure extent.

In other respects, better self-healing in the case of high temperatures and long healing periods can be attributed to sufficient inter-diffusion of polymer chains, which promotes epoxidation at the interphase [1, 19, 69]. Indeed, for Group 3 and Group 4 compounds comprising both lignin and CIMB, remarkably higher self-healing performance could be achieved at high temperatures when they are allowed to keep healing for sufficient healing time. However, it should be noted that healing efficiency tends to decrease at temperatures over 180 °C. The decrease in self-healing performance at 190 °C, can be associated with physical cross-links based on ionic interaction or hydrogen bonds [70].

3.4. Cross-link density

Cross-link densities of all the selected vulcanizates were calculated by using swelling results to understand better how self-healing performance is correlated to cross-link structure. Results are given in Table 5 for each compound, which was taken from the healing surfaces before and after self-healing. When evaluated, cross-link density values of the samples before self-healing are in a good correlation

Table 5. Swelling ratio (Q), cross-link density (V_c) and molecular weight between cross-links (M_c) of the vulcanizates based on swelling measurements.

	Before self-healing [mol/m ³]			After self-healing [mol/m ³]		
	Q [%]	V_c [mol/m ³]	$M_c \cdot 10^3$ [g/mol]	Q [%]	V_c [mol/m ³]	$M_c \cdot 10^3$ [g/mol]
REF	1.7±0.3	585±26	2.2±0.1	2.2±0.1	397±26	2.9±0.1
LA6	1.8±0.1	594±68	1.9±0.1	1.9±0.2	522±78	2.3±0.1
15CIMB	1.9±0.5	517±65	2.3±0.1	1.8±0.0	563±21	2.0±0.0
LA6-15CIMB	2.0±0.2	453±86	2.4±0.1	1.7±0.0	635±19	1.8±0.0

with their cure extent values given in Table 2, which refers to cure data. For 15CIMB and LA6-15CIMB samples, cross-link density values were measured higher after self-healing.

It is much more remarkable for the LA6-15CIMB sample, which contains both lignin and CIMB in higher amounts. It is very well-known that extent of cross-linking reaction of ENR strictly depends on the ring-opening level of the epoxy groups. Besides, the amount of lignin has a significant impact on the reaction by promoting the interaction between epoxy groups and CIMB. Therefore, the higher cross-link density of the given sample after self-healing can readily be attributed to further cross-linking reactions, and this finding supports the fact that LA6-15CIMB composition exhibits the best self-healing performance, as indicated above. This is also an expected result of decreasing average molecular weight between the cross-links (M_c). Indeed, the elastic retention force is inversely proportional to the average distance between the cross-links on the polymer chain [55, 73].

When we correlate with the initial cross-link density, self-healing performance has been found to decrease with increasing cross-link density due to less polymer chain diffusion in the rubber matrix, as extensively explained in related studies in the literature [21,

74, 75]. However, when the fractured samples are subjected to the self-healing process for appropriate healing conditions (time and temperature), further cross-links are able to form if the rubber compound contains the required species promoting self-healing [19, 21, 26, 72]. LA6-15CIMB sample, which has the lowest initial cross-link density and the highest one after self-healing, represents this fact as a good example.

3.5. Optical micrographs of self-healed materials

For all the compound groups, 180 °C – 15 min has been found to be the best self-healing condition. Thus, representative pictures of the samples, which were healed at 180 °C were given below in Figure 4. Healed samples were also shown under ×100 magnification in Figure 5. Figures clearly show that all the parameters: composition, temperature, and healing time, are highly effective in self-healing performance. Samples, which self-healed at appropriate conditions, could exhibit excellent recovery that is almost the same as their initial appearance. The sample exhibiting the highest self-healing ratio, LA6-15CIMB, has also been depicted in Figure 6 to verify how high self-healing performance affects physical appearance.

**Figure 4.** Representative pictures – original tensile-fractured samples before self-healing and after self-healing at 180 °C for 15 min.

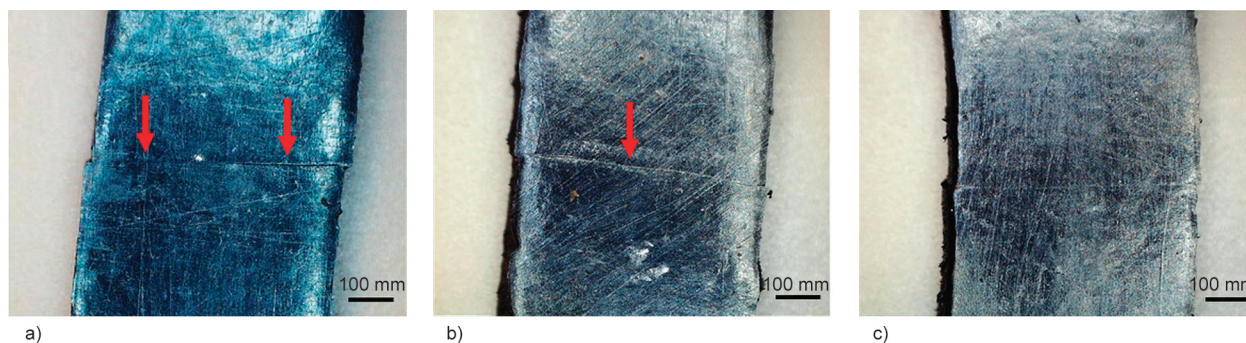


Figure 5. Optical micrographs of LA6-15CIMB samples after self-healing a) at 180 °C for 5 min, b) at 180 °C for 10 min, and c) at 180 °C for 15 min.



Figure 6. LA6-15CIMB sample after self-healing at 180 °C for 15 min.

3.6. FTIR analysis and proposed reaction mechanism

For verifying the potential chemical interactions between ENR, lignin, and CIMB, selected samples were analyzed by using an FTIR device. The attenuated total reflectance (ATR)-FTIR spectrum of the reference compound REF, LA6, 15CIMB, and LA6-15CIMB compounds are given in Figure 7 and Figure 8, respectively, before and after self-healing at 180 °C for 15 min healing conditions.

The peaks at 2959, 2917, and 2850 cm^{-1} in Figure 8, which are detected at all vulcanizate spectra, are characteristic peaks of ENR and represent $-\text{CH}_3$ stretching vibration, C–H stretching vibration, and $-\text{CH}_2$ symmetric and asymmetric stretching vibrations, respectively [76, 77]. Besides, the 875 cm^{-1} band refers to the presence of an epoxy ring (C–O–C) along with 1458 and 1377 cm^{-1} bands, which belong

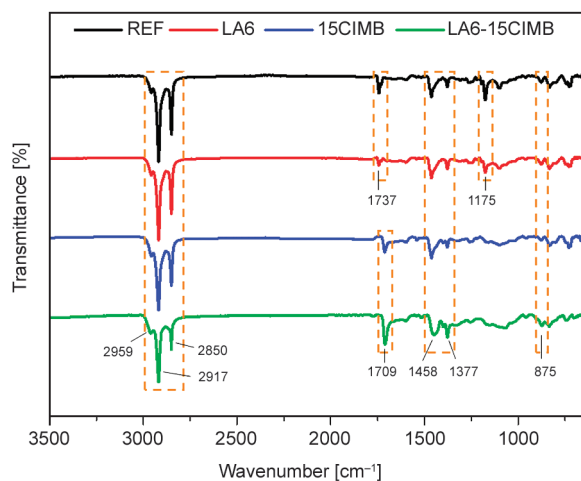


Figure 7. ATR-FTIR spectra of selected vulcanizates.

to C–H stretching and bending vibrations, respectively [1, 21, 56, 68, 77–81].

In Figure 7, the cyclic imide ($-\text{C}=\text{O}$) bending vibration peak, which is characteristic of CIMB, is seen for 15CIMB and LA6-15CIMB vulcanizates, as expected [61]. When comparing LA6 and REF samples, the peak intensity at 1175 cm^{-1} is lower for LA6 vulcanizates which refers to lignin to promote epoxy ring opening reaction in ENR [1, 82].

In Figure 8a and Figure 8b, for REF and LA6 compounds, the peaks around 1700 cm^{-1} (1737 and 1743 cm^{-1}) refer to non-conjugated C=O of carbonyl and carboxylic groups. These peaks are associated with the oxidation of cis-double bonds and/or the rearrangement of epoxy groups [1, 43, 78]. Higher peak intensity at 1097 and 1065 cm^{-1} bands in FTIR spectra of LA6 and LA6-15CIMB (Figure 8b and Figure 8d) indicates increasing C–O–C stretching vibrations. These peaks can be associated with the ENR backbone to interact with the other species present in the reaction media [6]. Besides, C=S and C=O groups come from epoxy ring opening reactions [80]. The

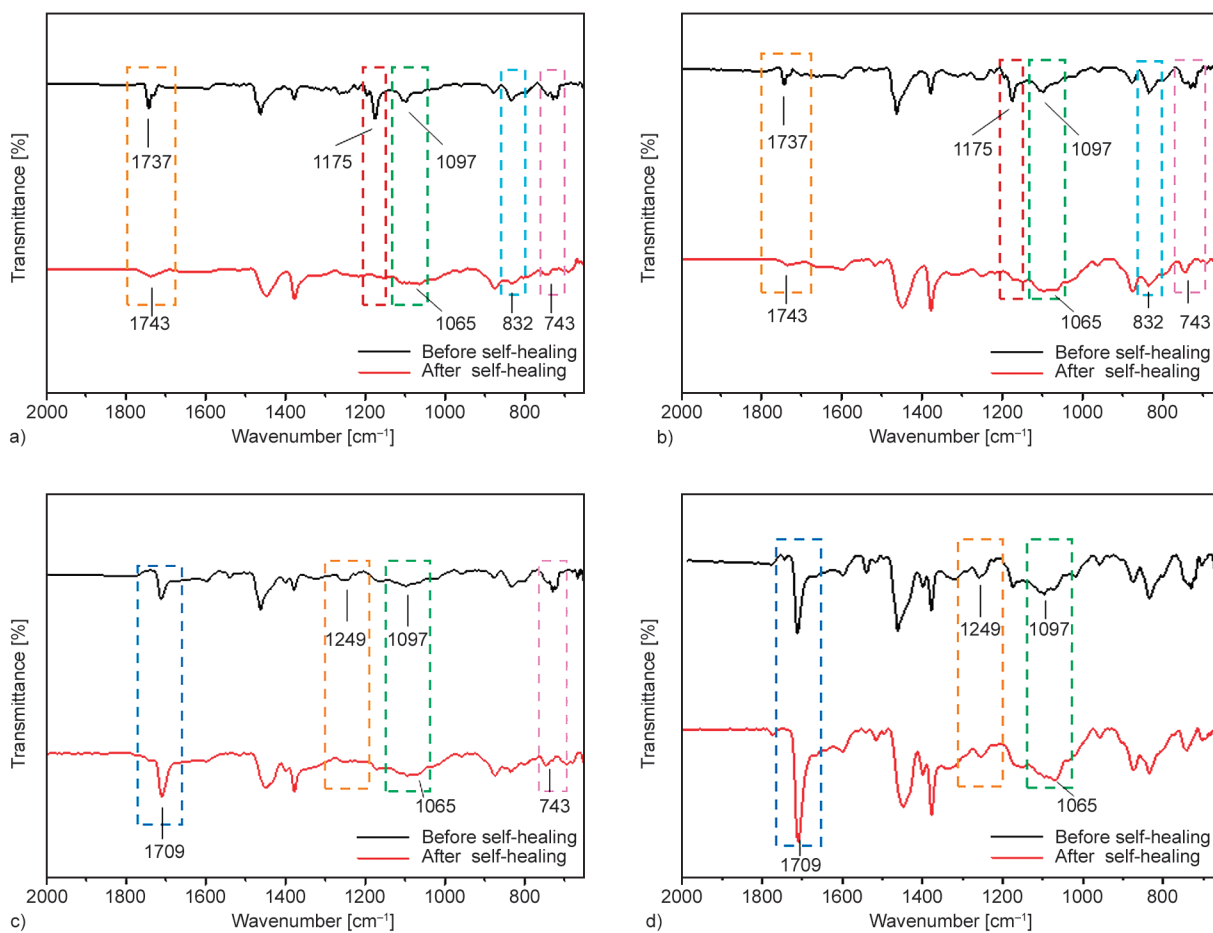


Figure 8. Extended ATR-FTIR spectra of a) REF, b) LA6, c) 15CIMB, and d) LA6-15CIMB vulcanizates before and after self-healing.

increasing peak intensity in the same absorption band also supports the presence of ether cross-links between lignin and epoxy groups of ENR as well as sulfonate ester cross-links [84]. Please note that the highest self-healing ratio of the LA6-15CIMB sample was also attributed to the possible chemical interactions between lignin, ENR, and CIMB. In [Figure 8a](#) and [Figure 8b](#), the peak intensity of the 832 cm^{-1} band refers to C=C bonds after self-healing. For all the samples, 1249 and 743 cm^{-1} bands belong to C–O symmetric stretching vibration and ring stretching vibration, respectively [1, 77, 83]. Then, the sharp decrease in the peak intensities of the same bands is attributed to the epoxy ring opening reaction for LA6-15CIMB vulcanizate.

CIMB is known to attach to the polymer structure via the broken cross-links during reversion, whereas it is normally not active at the beginning of the vulcanization reaction [28, 84]. In [Figure 7](#), cyclic imide (–C=O) stretching vibration peak (1709 cm^{-1}) is detected in the presence of CIMB. Cross-linking during self-healing is expected to occur via C=C bonds

on ENR for CIMB-containing vulcanizates [61]. This is also supported by the highly increasing 1709 cm^{-1} peak for LA6-15CIMB vulcanizate ([Figure 8c](#) and [Figure 8d](#)), which exhibits the best self-healing performance.

Evaluating all FTIR observations as well as the rheological and mechanical test results, the proposed reaction mechanism between ENR, lignin, and CIMB is summarized in [Figures 9–11](#). [Figure 9](#) depicts the traditional sulfur vulcanization of ENR and epoxy ring-opening reaction. During the vulcanization step at a sufficiently high vulcanization temperature, the active accelerator complex, which is able to react with sulfur, reacts with allylic sites of the polymer chain and readily initiates cross-linking reaction [85].

Also, the epoxy ring-opening reaction of ENR by the effect of lignin is given in [Figure 9](#). Kraft lignin is a branched macromolecule and is able to give strong intra-molecular interactions thanks to its several functionalities. Phenolic hydroxyl groups have the highest concentration among these functionalities

[47]. Reactive –OH groups of lignin interact with the oxygen atom on the ENR epoxy ring to initiate the ring-opening reaction via the formation of hydrogen bonding [4]. Cross-linking reaction between ENR and lignin without using any curative has also been well-defined in literature [45].

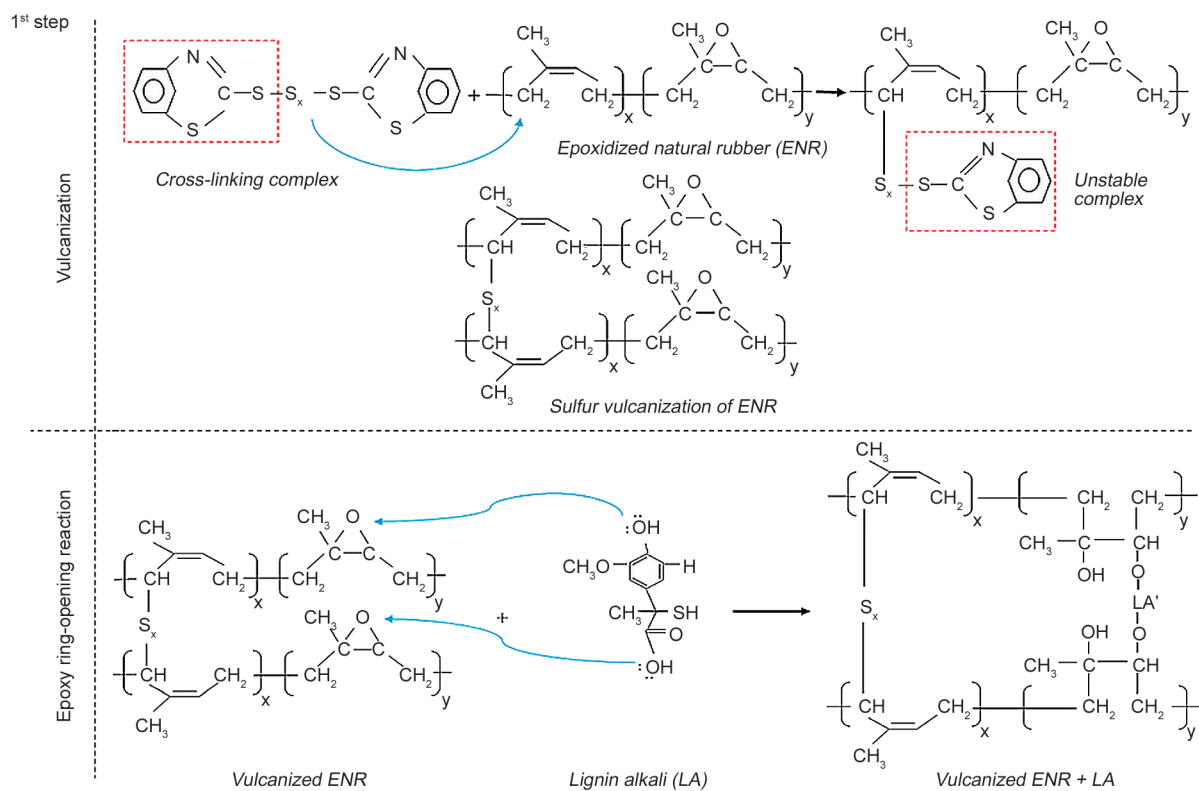


Figure 9. Traditional sulfur vulcanization mechanism and the epoxy ring-opening reaction of ENR in the presence of lignin.

2nd step: Diels-Alder and retro Diels-Alder reaction between ENR and CIMB

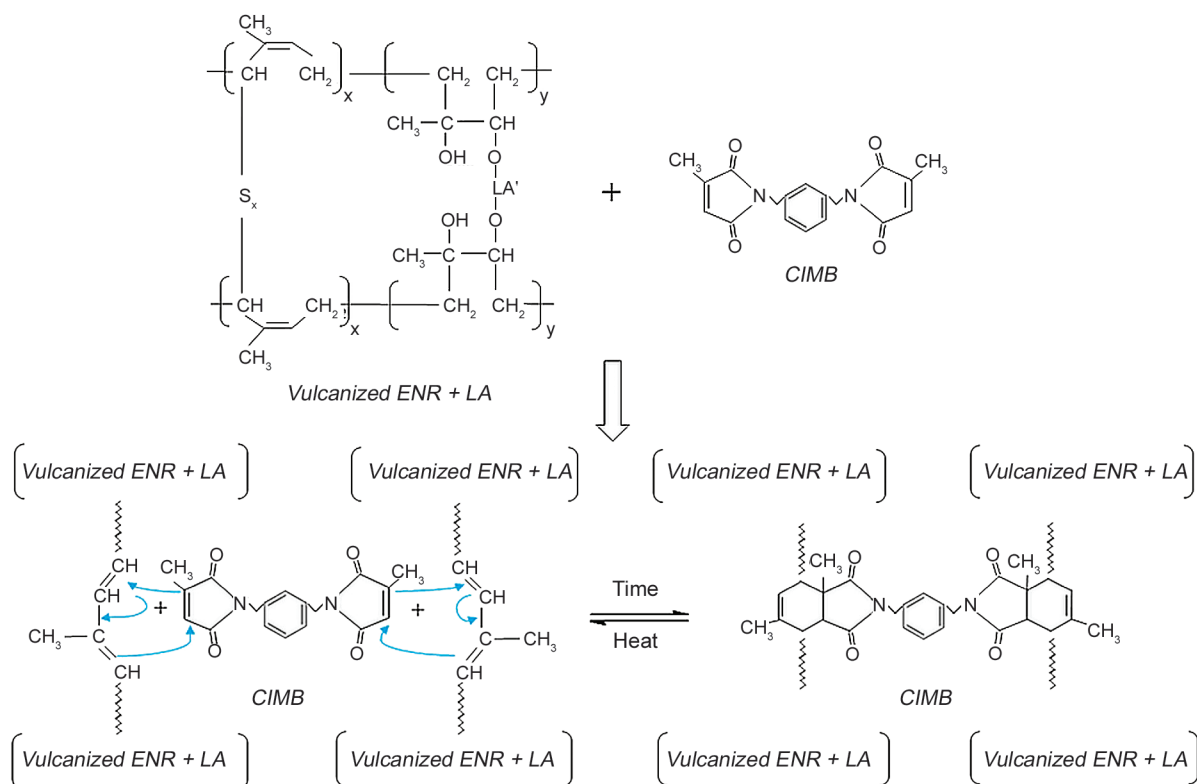


Figure 10. Proposed Diels-Alder and retro-Diels-Alder reaction mechanisms between ENR and CIMB.

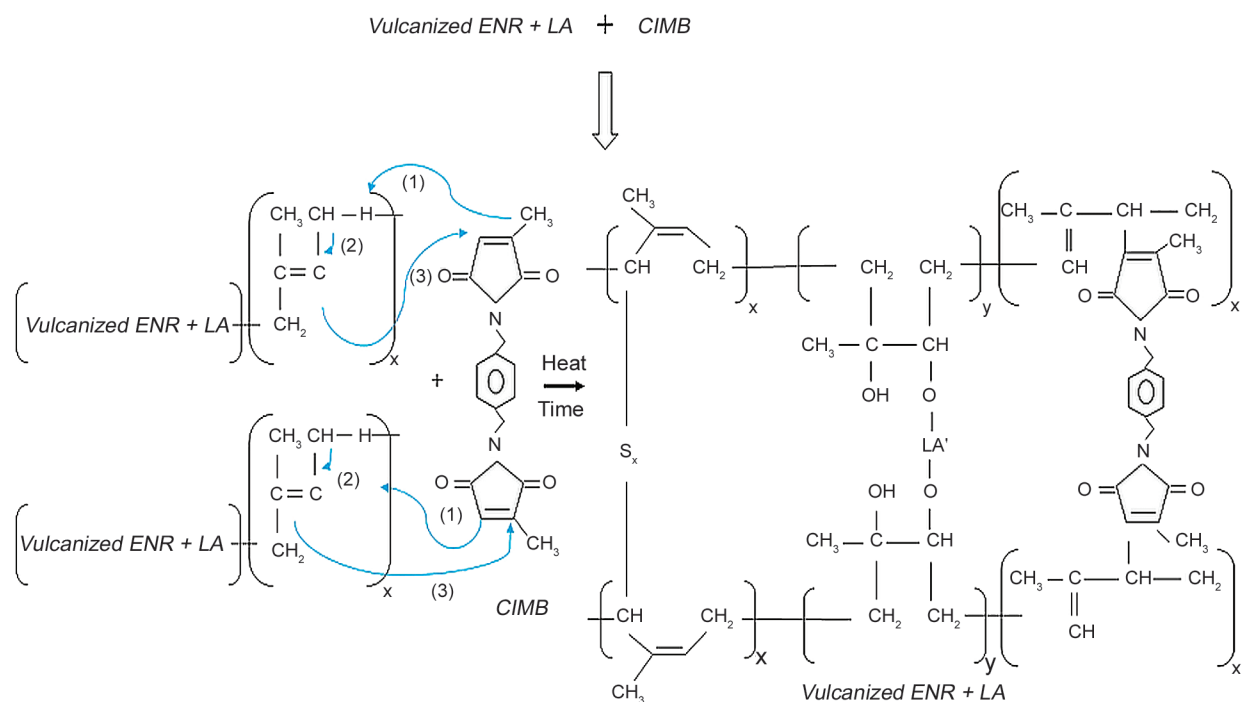
3rd step: Alder-ene reaction between ENR and CIMB

Figure 11. Proposed Alder-ene reaction between ENR and CIMB.

CIMB is a traditional anti-reversion agent, which is able to interact with double bonds on the polymer chain to provide reversible covalent bonds via a Diels-Alder reaction at relatively high vulcanization temperatures. Therefore, CIMB can be considered as a potential self-healing agent for sulfur-cured rubber materials [29, 60, 84]. The amount of reversible cross-links depends on double bond concentration on the polymer backbone, as expected. For ENR vulcanizates, along with the double bonds, epoxy rings have the potential to increase total reactivity for interacting with CIMB molecules.

In this study, the main function of lignin is believed to promote the epoxy ring-opening reaction to let ENR interact further with CIMB. The proposed Diels-Alder reaction mechanism of ENR in the presence of both lignin and CIMB is given in Figure 10. Carbonyl groups linked to maleimide terminations make the double bond on bismaleimide highly active to act as a dienophile for the Diels-Alder reaction with conjugated dienes [30]. Increasing cross-link density of LA6-15CIMB vulcanizate after self-healing also coincides with the diene-dienophile reaction (Diels-Alder) of CIMB and double bonds on fractured polymer chains [29, 37, 86, 87].

The proposed Alder-ene reaction mechanism between CIMB and isoprene units on ENR molecules is given in Figure 11 [30, 61, 62]. This reaction is

thought to take place within the self-healing process. Higher cross-link density of CIMB containing vulcanizates after self-healing, as well as new chemical bonds detected in FTIR spectra of these samples, can be accepted as strong proof for this evaluation.

3.7. Dynamic mechanical analysis

The reversible character of the self-healing process was investigated by following the dynamic modulus of the four representative samples. The selected vulcanizates REF, LA6, 15CIMB, and LA6-15CIMB, which were already self-healed at 180 °C for 15 min, were subjected to customized dynamic heating-cooling cycles, and the obtained results are given in Figure 12. In each cycle of dynamic analysis, the retro-Diels-Alder reaction is expected to occur at high temperatures, whereas the ENR and CIMB give Diels-Alder reaction during cooling down to 40 °C. As seen in the figure, storage modulus, as well as loss modulus values, increase in the cooling period indicating the Diels-Alder reaction as well as the Alder-ene reaction in each cycle. Immediately after the heating period starts, the modulus values show a sharp drop. This behavior can be attributed to the retro-Diels-Alder reaction, which results in breaking down the cross-links formed by Diels-Alder and Alder-ene reactions in the previous cooling period, and the overall dynamic results show a good correlation with

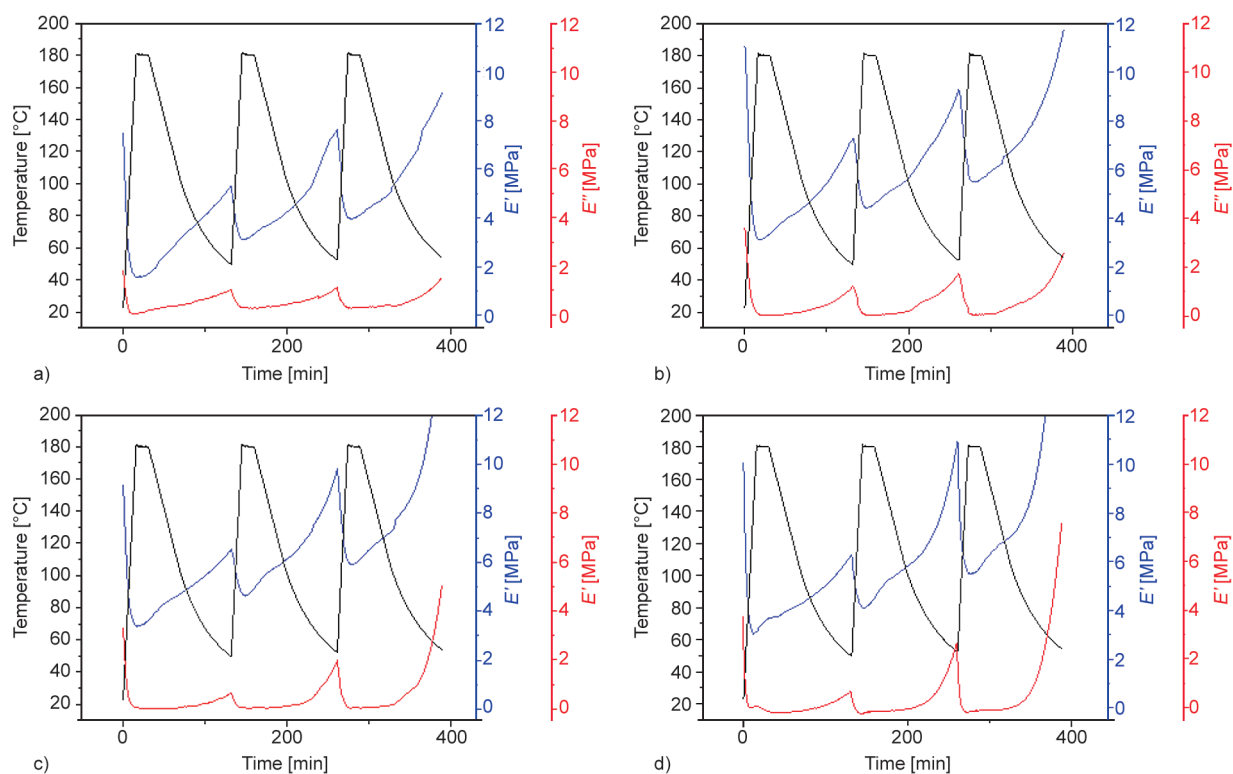


Figure 12. Dynamic moduli of the selected vulcanizates during repetitive heating-cooling cycles. a) REF, b) LA6, c) 15CIMB and d) LA6-15CIMB.

the recent literature [8, 26, 88]. When we compare the storage modulus of lignin and CIMB-containing samples with the reference one, significantly higher modulus values of these samples after each cooling period were also found to be related to their higher self-healing ratio. Besides, the LA6-15CIMB compound, which exhibited the highest level of healing, has the highest storage modulus values, especially after the second and third cycles. Indeed, the lower modulus of all CIMB-containing vulcanizates after the first cycle could easily be attributed to their lower initial mechanical strength.

4. Conclusions

In this study, the self-healing performance of an ENR-based rubber compound in the presence of lignin and CIMB has been investigated by means of retention in tensile strength as well as by visual inspection. Self-healing agents resulted in a higher cure rate due to reactive interactions of lignin and CIMB on the ENR matrix to promote further cross-linking reactions. Lignin could improve self-healing from 27 to 47% on its own, whereas CIMB, which was found to improve healing by balancing healing

and reversion processes, could do it up to 55% at specific healing conditions. Using 6 phr lignin and 15 phr CIMB in the same composition provided a remarkable increase in cross-link density by self-healing as well as the highest level of self-healing (83%) at 180 °C for 15 min healing time. This impressive healing ratio was attributed to the synergistic effect of lignin and CIMB at the best stoichiometric ratio. However, using any of lignin and CIMB may need further attention when the initial mechanical properties are of interest since both additives have an adverse effect on the mechanical strength of the ENR-based material.

The reaction mechanism comprising lignin-promoted epoxy ring-opening reaction on ENR backbone, Diels-Alder, and Alder-ene reactions between CIMB and isoprene units of ENR was proposed for the self-healing process. The reversible character of Diels-Alder and retro-Diels-Alder reactions could also be proved by dynamic analysis.

Acknowledgements

The authors gratefully thank TÜBİTAK (Project no: 221M572) for financial support.

References

- [1] Rahman M. A., Sartore L., Bignotti F., di Landro L.: Autonomic self-healing in epoxidized natural rubber. *ACS Applied Materials and Interfaces*, **5**, 1494–1502 (2013).
<https://doi.org/10.1021/am303015e>
- [2] Khan A. A. P., Khan A., Ansari O., Shaban M., Rub M. A., Azum N., Jilani A., Asiri A. M.: Self-healing of polymer materials and their composites. in ‘Self-healing composite materials’ (eds.: Khan A., Jawaid M., Raveendran S. N., Asiri A. M. A.) 103–121 (2019).
<https://doi.org/10.1016/B978-0-12-817354-1.00007-7>
- [3] Zhu M., Liu J., Gan L., Long M.: Research progress in bio-based self-healing materials. *European Polymer Journal*, **129**, 109651 (2020).
<https://doi.org/10.1016/j.eurpolymj.2020.109651>
- [4] Behera P. K., Mohanty S., Gupta V. K.: Self-healing elastomers based on conjugated diolefins: A review. *Polymer Chemistry*, **12**, 1598–1621 (2021).
<https://doi.org/10.1039/d0py01458c>
- [5] Terryn S., Langenbach J., Roels E., Brancart J., Bakkali-Hassani C., Poutrel Q., Georgopoulou A., Thuruthel T. G., Safaei A., Ferrentino P., Sebastian T., Norvez S., Iida F., Bosman A. W., Tournilhac F., Clemens F., van Assche G., Vanderborght B.: A review on self-healing polymers for soft robotics. *Materials Today*, **47**, 187–205 (2021).
<https://doi.org/10.1016/j.mattod.2021.01.009>
- [6] Xu C., Nie J., Wu W., Fu L., Lin B.: Design of self-healable supramolecular hybrid network based on carboxylated styrene butadiene rubber and nano-chitosan. *Carbohydrate Polymers*, **205**, 410–419 (2019).
<https://doi.org/10.1016/j.carbpol.2018.10.080>
- [7] Utrera-Barrios S., Verdejo R., López-Manchado M. A., Santana M. H.: Evolution of self-healing elastomers, from extrinsic to combined intrinsic mechanisms: A review. *Materials Horizons*, **7**, 2882–2902 (2020).
<https://doi.org/10.1039/d0mh00535e>
- [8] Utrera-Barrios S., Verdejo R., López-Manchado M. A., Santana M. H.: The final frontier of sustainable materials: Current developments in self-healing elastomers. *International Journal of Molecular Sciences*, **23**, 4757 (2022).
<https://doi.org/10.3390/ijms23094757>
- [9] Ismail H.: Potential of rubberwood as a filler in epoxidized natural rubber compounds. *Journal of Elastomers and Plastics*, **33**, 34–46 (2001).
<https://doi.org/10.1106/B04H-YKPD-H80B-KQ8N>
- [10] Mascia L., Clarke J., Ng K. S., Chua K. S., Russo P.: Cure efficiency of dodecyl succinic anhydride as a cross-linking agent for elastomer blends based on epoxidized natural rubber. *Journal of Applied Polymer Science*, **132**, 41448 (2015).
<https://doi.org/10.1002/app.41448>
- [11] Tanjung F. A., Hassan A., Hasan M.: Use of epoxidized natural rubber as a toughening agent in plastics. *Journal of Applied Polymer Science*, **132**, 42270 (2015).
<https://doi.org/10.1002/app.42270>
- [12] Luo Y. Y., Wang Y. Q., Zhong J. P., He C. Z., Li Y. Z., Peng Z.: Interaction between fumed-silica and epoxidized natural rubber. *Journal of Inorganic and Organometallic Polymers and Materials*, **21**, 777–783 (2011).
<https://doi.org/10.1007/s10904-011-9539-x>
- [13] Poh B. T., Lim A. L.: Adhesion properties of pressure-sensitive adhesives prepared from SMR 10/ENR 25, SMR 10/ENR 50, and ENR 25/ENR 50 blends. *Journal of Applied Polymer Science*, **109**, 115–119 (2008).
<https://doi.org/10.1002/app.27489>
- [14] Xu T., Jia Z., Wang S., Chen Y., Luo Y., Jia D., Peng Z.: Self-crosslinkable epoxidized natural rubber–silica hybrids. *Journal of Applied Polymer Science*, **134**, 44605 (2017).
<https://doi.org/10.1002/app.44605>
- [15] Öter M., Karağaç B.: Epoxidised natural rubber as adhesion promoter in natural rubber based compounds. *Journal of Rubber Research*, **23**, 333–341 (2020).
<https://doi.org/10.1007/s42464-020-00061-9>
- [16] Roychoudhury A., De P. P., Bhowmick A. K., De S. K.: Self-crosslinkable ternary blend of chlorosulphonated polyethylene, epoxidized natural rubber and carboxylated nitrile rubber. *Polymer*, **33**, 4737–4740 (1992).
[https://doi.org/10.1016/0032-3861\(92\)90686-Q](https://doi.org/10.1016/0032-3861(92)90686-Q)
- [17] Cheng B., Lu X., Zhou J., Qin R., Yang Y.: Dual cross-linked self-healing and recyclable epoxidized natural rubber based on multiple reversible effects. *ACS Sustainable Chemistry and Engineering*, **7**, 4443–4455 (2019).
<https://doi.org/10.1021/acssuschemeng.8b06437>
- [18] Ünügül T., Karağaç B.: Vulcanization of chlorinated polyethylene/chloroprene rubber compounds at lower temperatures in the presence of reactive silanes. *Journal of Applied Polymer Science*, **138**, 50544 (2021).
<https://doi.org/10.1002/app.50544>
- [19] Imbernon L., Oikonomou E. K., Norvez S., Leibler L.: Chemically crosslinked yet reprocessable epoxidized natural rubber *via* thermo-activated disulfide rearrangements. *Polymer Chemistry*, **6**, 4271–4278 (2015).
<https://doi.org/10.1039/c5py00459d>
- [20] Liu L., Zhu L., Zhang L.: A solvent-resistant and biocompatible self-healing supramolecular elastomer with tunable mechanical properties. *Macromolecular Chemistry and Physics*, **219**, 1700409 (2018).
<https://doi.org/10.1002/macp.201700409>
- [21] Xu C., Nie J., Wu W., Zheng Z., Chen Y.: Self-healable, recyclable, and strengthened epoxidized natural rubber/carboxymethyl chitosan biobased composites with hydrogen bonding supramolecular hybrid networks. *ACS Sustainable Chemistry and Engineering*, **7**, 15778–15789 (2019).
<https://doi.org/10.1021/acssuschemeng.9b04324>
- [22] Algaily B., Kaewsakul W., Sarkawi S. S., Kalkornsurapranee E.: A self-healing system based on ester crosslinks for carbon black-filled rubber compounds. *Journal of Composites Science*, **5**, 70 (2021).
<https://doi.org/10.3390/jcs5030070>

- [23] Wu D. Y., Meure S., Solomon D.: Self-healing polymeric materials: A review of recent developments. *Progress in Polymer Science*, **33**, 479–522 (2008).
<https://doi.org/10.1016/j.progpolymsci.2008.02.001>
- [24] Boden J., Bowen C. R., Buchard A., Davidson M. G., Norris C.: Understanding the effects of cross-linking density on the self-healing performance of epoxidized natural rubber and natural rubber. *ACS Omega*, **7**, 15098–15105 (2022).
<https://doi.org/10.1021/acsomega.2c00971>
- [25] Gheneim R., Perez-Berumen C., Gandini A.: Diels–Alder reactions with novel polymeric dienes and dienophiles: Synthesis of reversibly cross-linked elastomer. *Macromolecules*, **35**, 7246–7253 (2002).
<https://doi.org/10.1021/ma020343c>
- [26] Tanasi P., Santana M. H., Carretero-González J., Verdejo R., López-Manchado M. A.: Thermo-reversible cross-linked natural rubber: A Diels–Alder route for reuse and self-healing properties in elastomers. *Polymer*, **175**, 15–24 (2019).
<https://doi.org/10.1016/j.polymer.2019.04.059>
- [27] Wemyss A. M., Bowen C., Plesse C., Vancaeyzeele C., Nguyen G. T. M., Vidal F., Wan C.: Dynamic crosslinked rubbers for a green future: A material perspective. *Materials Science and Engineering R: Reports*, **141**, 100561 (2020).
<https://doi.org/10.1016/j.mser.2020.100561>
- [28] Sathi S. G., Jang J. Y., Jeong K-U., Nah C.: Thermally stable bromobutyl rubber with a high crosslinking density based on a 4,4'-bismaleimidodiphenylmethane curing agent. *Journal of Applied Polymer Science*, **133**, 44092 (2016).
<https://doi.org/10.1002/app.44092>
- [29] Gopi Sathi S., Stoček R., Kratina O.: Reversion free high-temperature vulcanization of cis-polybutadiene rubber with the accelerated-sulfur system. *Express Polymer Letters*, **14**, 823–837 (2020).
<https://doi.org/10.3144/expresspolymlett.2020.68>
- [30] Sathi G. S., Jeon J., Won J., Nah C.: Enhancing the efficiency of zinc oxide vulcanization in brominated poly (isobutylene-co-isoprene) rubber using structurally different bismaleimides. *Journal of Polymer Research*, **25**, 108 (2018).
<https://doi.org/10.1007/s10965-018-1512-8>
- [31] Mishra S., Mohanty A. K., Drzal L. T., Misra M., Hinrichsen G.: A review on pineapple leaf fibers, sisal fibers and their biocomposites. *Macromolecular Materials and Engineering*, **289**, 955–974 (2004).
<https://doi.org/10.1002/mame.200400132>
- [32] Aradoaei S., Darie R., Constantinescu G., Olariu M., Ciobanu R.: Modified lignin effectiveness as compatibilizer for PET/LDPE blends containing secondary materials. *Journal of Non-Crystalline Solids*, **356**, 768–771 (2010).
<https://doi.org/10.1016/j.jnoncrysol.2009.11.046>
- [33] Asrul M., Othman M., Zakaria M., Fauzi M. S.: Lignin filled unvulcanised natural rubber latex: Effects of lignin on oil resistance, tensile strength and morphology of rubber films. *International Journal of Engineering Science Invention*, **2**, 38–43 (2013).
- [34] Kakroodi A. R., Rodrigue D.: Degradation behavior of maleated polyethylene/ground tire rubber thermoplastic elastomers with and without stabilizers. *Polymer Degradation and Stability*, **98**, 2184–2192 (2013).
<https://doi.org/10.1016/j.polymdegradstab.2013.08.017>
- [35] Thakur V. K., Thakur M. K., Raghavan P., Kessler M. R.: Progress in green polymer composites from lignin for multifunctional applications: A review. *ACS Sustainable Chemistry and Engineering*, **2**, 1072–1092 (2014).
<https://doi.org/10.1021/sc500087z>
- [36] Phakkeeree T., Ikeda Y., Yokohama H., Phinyocheep P., Kitano R., Kato A.: Network-like structure of lignin in natural rubber matrix to form high performance elastomeric bio-composite. *Journal of Fiber Science and Technology*, **72**, 160–165 (2016).
<https://doi.org/10.2115/fiberst.fiberst.2016-0023>
- [37] Zhou W., Zhang H., Chen F.: Modified lignin: Preparation and use in reversible gel *via* Diels–Alder reaction. *International Journal of Biological Macromolecules*, **107**, 790–795 (2018).
<https://doi.org/10.1016/j.ijbiomac.2017.09.052>
- [38] Yu P., He H., Jia Y., Tian S., Chen J., Jia D., Luo Y.: A comprehensive study on lignin as a green alternative of silica in natural rubber composites. *Polymer Testing*, **54**, 176–185 (2016).
<https://doi.org/10.1016/j.polymertesting.2016.07.014>
- [39] Doherty W. O. S., Mousavioun P., Fellows C. M.: Value-adding to cellulosic ethanol: Lignin polymers. *Industrial Crops and Products*, **33**, 259–276 (2011).
<https://doi.org/10.1016/j.indcrop.2010.10.022>
- [40] Mili M., Hashmi S. A. R., Ather M., Hada V., Markandeya N., Kamble S., Mohapatra M., Rathore S. K. S., Srivastava A. K., Verma S.: Novel lignin as natural-biodegradable binder for various sectors – A review. *Journal of Applied Polymer Science*, **139**, 51951 (2021).
<https://doi.org/10.1002/app.51951>
- [41] Frigerio P., Zoia L., Orlandi M., Hanel T., Castellani L.: Application of sulphur-free lignins as a filler for elastomers: Effect of hexamethylenetetramine treatment. *BioResources*, **9**, 1387–1400 (2021).
- [42] Makhalema M., Hlangothi P., Motloung S. V., Koao L. F., Motaung T. E.: Influence of kraft lignin on the properties of rubber composites. *Wood Research*, **66**, 285–296 (2021).
<https://doi.org/10.37763/wr.1336-4561/66.2.285296>
- [43] Barana D., Ali S. D., Salanti A., Orlandi M., Castellani L., Hanel T., Zoia L.: Influence of lignin features on thermal stability and mechanical properties of natural rubber compounds. *ACS Sustainable Chemistry and Engineering*, **4**, 5258–5267 (2016).
<https://doi.org/10.1021/acsschemeng.6b00774>

- [44] Moreno A., Sipponen M. H.: Lignin-based smart materials: A Roadmap to processing and synthesis for current and future applications. *Materials Horizons*, **7**, 2237–2257 (2020)
<https://doi.org/10.1039/d0mh00798f>
- [45] Jiang C., He H., Yao X., Yu P., Zhou L., Jia D.: Self-crosslinkable lignin/epoxidized natural rubber composites. *Journal of Applied Polymer Science*, **131**, 41166 (2014).
<https://doi.org/10.1002/app.41166>
- [46] Sakunkittiyut Y., Kunanopparat T., Menut P., Siri wattanayotin S.: Effect of kraft lignin on protein aggregation, functional, and rheological properties of fish protein-based material. *Journal of Applied Polymer Science*, **127**, 1703–1710 (2013).
<https://doi.org/10.1002/app.37899>
- [47] Laurichesse S., Avérous L.: Chemical modification of lignins: Towards biobased polymers. *Progress in Polymer Science*, **39**, 1266–1290 (2014).
<https://doi.org/10.1016/j.progpolymsci.2013.11.004>
- [48] Chung H., Washburn N. R.: Extraction and types of lignin. in ‘Lignin in polymer composites’ (eds.: Faruk O., Sain M.) Elsevier, Amsterdam, 13–25 (2016).
<https://doi.org/10.1016/B978-0-323-35565-0.00002-3>
- [49] Mandlekar N., Cayla A., Rault F., Giraud S., Salaün F., Malucelli G., Guan J-P.: An overview on the use of lignin and its derivatives in fire retardant polymer systems. in ‘Lignin – Trends and applications’ (ed.: Poletto M.) 207–231 (2018).
<https://doi.org/10.5772/intechopen.72963>
- [50] Gosselink R. J. A., Snijder M. H. B., Kranenbarg A., Keijsers E. R. P., de Jong E., Stigsson L. L.: Characterisation and application of NovaFiber lignin. *Industrial Crops and Products*, **20**, 191–203 (2004).
<https://doi.org/10.1016/j.indcrop.2004.04.021>
- [51] Ikeda Y., Phakkeeree T., Junkong P., Yokohama H., Phinyocheep P., Kitano R., Kato A.: Reinforcing biofiller ‘Lignin’ for high performance green natural rubber nanocomposites. *RSC Advances*, **7**, 5222–5231 (2017).
<https://doi.org/10.1039/c6ra26359c>
- [52] Duval A., Lange H., Lawoko M., Crestini C.: Reversible crosslinking of lignin *via* the furan-maleimide Diels-Alder reaction. *Green Chemistry*, **17**, 4991–5000 (2015).
<https://doi.org/10.1039/c5gc01319d>
- [53] Hernández M., Grande A. M., Dierkes W., Bijleveld J., van der Zwaag S., García S. J.: Turning vulcanized natural rubber into a self-healing polymer: Effect of the disulfide/polysulfide ratio. *ACS Sustainable Chemistry and Engineering*, **4**, 5776–5784 (2016).
<https://doi.org/10.1021/acssuschemeng.6b01760>
- [54] Khimi S., Syamsinar S. N., Najwa T. N. L.: Effect of carbon black on self-healing efficiency of natural rubber. *Materials Today: Proceedings*, **17**, 1064–1071 (2019).
<https://doi.org/10.1016/j.matpr.2019.06.513>
- [55] Flory P. J., Rehner J.: Statistical mechanics of cross-linked polymer networks II. Swelling. *The Journal of Chemical Physics*, **11**, 521–526 (1943)
<https://doi.org/10.1063/1.1723792>
- [56] Cao L., Fan J., Huang J., Chen Y.: A robust and stretchable cross-linked rubber network with recyclable and self-healable capabilities based on dynamic covalent bonds. *Journal of Materials Chemistry A*, **7**, 4922–4933 (2019).
<https://doi.org/10.1039/c8ta11587g>
- [57] Jiang G., Zhang J., Ding J., Chen Y.: Design of PLA/ENR thermoplastic vulcanizates with balanced stiffness-toughness based on rubber reinforcement and selective distribution of modified silica. *Polymers for Advanced Technologies*, **32**, 2487–2498 (2021).
<https://doi.org/10.1002/pat.5279>
- [58] Somseemee O., Saeoui P., Schevenels F. T., Siriwong C.: Enhanced interfacial interaction between modified cellulose nanocrystals and epoxidized natural rubber *via* ultraviolet irradiation. *Scientific Reports*, **12**, 6682 (2022).
<https://doi.org/10.1038/s41598-022-10558-5>
- [59] Menon A. R. R., Pillai C. K. S., Nando G. B.: Vulcanization of natural rubber modified with cashew nut shell liquid and its phosphorylated derivative – A comparative study. *Polymer*, **39**, 4033–4036 (1998).
[https://doi.org/10.1016/S0032-3861\(97\)00539-9](https://doi.org/10.1016/S0032-3861(97)00539-9)
- [60] Karaağaç B.: Use of ground pistachio shell as alternative filler in natural rubber/styrene-butadiene rubber-based rubber compounds. *Polymer Composites*, **35**, 245–252 (2014).
<https://doi.org/10.1002/pc.22656>
- [61] Monsallier J. M.: Multifunctional acrylates as anti-reversion agents in sulfur cured systems. *Kautschuk Gummi Kunststoffe*, **62**, 442–447 (2009).
- [62] Shibulal G. S., Jang J., Yu H. C., Huh Y. I., Nah C.: Cure characteristics and physico-mechanical properties of a conventional sulphur-cured natural rubber with a novel anti-reversion agent. *Journal of Polymer Research*, **23**, 237 (2016).
<https://doi.org/10.1007/s10965-016-1128-9>
- [63] Gopi Sathi S., Harea E., Machů A., Stoček R.: Facilitating high-temperature curing of natural rubber with a conventional accelerated-sulfur system using a synergistic combination of bismaleimides. *Express Polymer Letters*, **15**, 16–27 (2021).
<https://doi.org/10.3144/expresspolymlett.2021.3>
- [64] Hashim A. S., Kohjiya S.: Preparation and properties of epoxidized natural rubber network crosslinked by ring opening reaction. *Polymer Gels and Networks*, **2**, 219–227 (1994).
[https://doi.org/10.1016/0966-7822\(94\)90006-X](https://doi.org/10.1016/0966-7822(94)90006-X)
- [65] Zurina M., Ismail H., Ratnam C. T.: The effect of HVA-2 on properties of irradiated epoxidized natural rubber (ENR-50), ethylene vinyl acetate (EVA), and ENR-50/EVA blend. *Polymer Testing*, **27**, 480–490 (2008).
<https://doi.org/10.1016/j.polymertesting.2008.02.001>
- [66] Aini N. A. M., Othman N., Hussin M. H., Sahakaro K., Hayemasae N.: Lignin as alternative reinforcing filler in the rubber industry: A review. *Frontiers in Materials*, **6**, 329 (2020).
<https://doi.org/10.3389/fmats.2019.00329>

- [67] Yang Z., Peng H., Wang W., Liu T.: Crystallization behavior of poly(ϵ -caprolactone)/layered double hydroxide nanocomposites. *Journal of Applied Polymer Science*, **116**, 2658–2667 (2010).
<https://doi.org/10.1002/app.31787>
- [68] Utrera-Barrios S., Araujo-Morera J., de los Reyes L. P., Manzanares V. R., Verdejo R., López-Manchado M. Á., Santana M. H.: An effective and sustainable approach for achieving self-healing in nitrile rubber. *European Polymer Journal*, **139**, 110032 (2020).
<https://doi.org/10.1016/j.eurpolymj.2020.110032>
- [69] Rahman M. A., Penco M., Peroni I., Ramorino G., Grande A. M., di Landro L.: Self-repairing systems based on ionomers and epoxidized natural rubber blends. *ACS Applied Materials and Interfaces*, **3**, 4865–4874 (2011).
<https://doi.org/10.1021/am201417h>
- [70] Pire M., Norvez S., Iliopoulos I., le Rossignol B., Leibler L.: Epoxidized natural rubber/dicarboxylic acid self-vulcanized blends. *Polymer*, **51**, 5903–5909 (2010).
<https://doi.org/10.1016/j.polymer.2010.10.023>
- [71] Araujo-Morera J., Santana M. H., Verdejo R., López-Manchado M. A.: Giving a second opportunity to tire waste: An alternative path for the development of sustainable self-healing styrene-butadiene rubber compounds overcoming the magic triangle of tires. *Polymers*, **11**, 2122 (2019).
<https://doi.org/10.3390/polym11122122>
- [72] Surendran A., Thomas S.: Self-healing polymer-based systems. Elsevier, Amsterdam (2020).
- [73] Moore C. G., Watson W. F.: Determination of degree of crosslinking in natural rubber vulcanizates. Part II. *Journal of Polymer Science*, **19**, 237–254 (1959).
<https://doi.org/10.1002/pol.1956.120199202>
- [74] Peng Y., Hou Y., Wu Q., Ran Q., Huang G., Wu J.: Thermal and mechanical activation of dynamically stable ionic interaction toward self-healing strengthening elastomers. *Materials Horizons*, **8**, 2553–2561 (2021).
<https://doi.org/10.1039/d1mh00638j>
- [75] Thajudin N. L. N., Zainol M. H., Shuib R. K.: Intrinsic room temperature self-healing natural rubber based on metal thiolate ionic network. *Polymer Testing*, **93**, 106975 (2021).
<https://doi.org/10.1016/j.polymertesting.2020.106975>
- [76] Salehabadi A., Bakar M. A., Bakar N. H. H. A.: Effect of organo-modified nanoclay on the thermal and bulk structural properties of poly(3-hydroxybutyrate)-epoxidized natural rubber blends: Formation of multi-components biobased nanohybrids. *Materials*, **7**, 4508–4523 (2014).
<https://doi.org/10.3390/ma7064508>
- [77] Tan W. L., Salehabadi A., Mohd Isa M. H., Abu Bakar M., Abu Bakar N. H. H.: Synthesis and physicochemical characterization of organomodified halloysite/epoxidized natural rubber nanocomposites: A potential flame-resistant adhesive. *Journal of Materials Science*, **51**, 1121–1132 (2016).
<https://doi.org/10.1007/s10853-015-9443-9>
- [78] Ratnam C. T., Nasir M., Baharin A., Zaman K.: Electron beam irradiation of epoxidized natural rubber. *Nuclear Instruments and Methods in Physics Research, Section B: Beam Interactions with Materials and Atoms*, **171**, 455–464 (2000).
[https://doi.org/10.1016/S0168-583X\(00\)00301-3](https://doi.org/10.1016/S0168-583X(00)00301-3)
- [79] Hamzah R., Bakar M. A., Khairuddean M., Mohammed I. A., Adnan R.: A structural study of epoxidized natural rubber (ENR-50) and its cyclic dithiocarbonate derivative using NMR spectroscopy techniques. *Molecules*, **17**, 10974–10993 (2012).
<https://doi.org/10.3390/molecules170910974>
- [80] Nie J., Mou W., Ding J., Chen Y.: Bio-based epoxidized natural rubber/chitin nanocrystals composites: Self-healing and enhanced mechanical properties. *Composites Part B*, **172**, 152–160 (2019).
<https://doi.org/10.1016/j.compositesb.2019.04.035>
- [81] Damampai K., Pichaiyut S., Mandal S., Wießner S., Das A., Nakason C.: Internal polymerization of epoxy group of epoxidized natural rubber by ferric chloride and formation of strong network structure. *Polymers*, **13**, 4145 (2021).
<https://doi.org/10.3390/polym13234145>
- [82] Jiang C., He H., Jiang H., Ma L., Jia D. M.: Nano-lignin filled natural rubber composites: Preparation and characterization. *Express Polymer Letters*, **7**, 480–493 (2013).
<https://doi.org/10.3144/expresspolymlett.2013.44>
- [83] Manoj N. R., De P. P., De S. K., Peiffer D. G.: Self-crosslinkable blend of zinc-sulfonated EPDM and epoxidized natural rubber. *Journal of Applied Polymer Science*, **53**, 361–370 (1994).
<https://doi.org/10.1002/app.1994.070530314>
- [84] Datta R. N., Ingham F. A. A.: High temperature curing of passenger tires by using 1,3-bis-(citraconimidomethyl) benzene. *Kautschuk und Gummi Kunststoffe*, **52**, 758–762 (1999).
- [85] Coran A. Y.: Vulcanization. in ‘Science and technology of rubber’ (eds.: Mark J. E., Erman B., Eirich F. R.) Academic Press, Cambridge, 321–366 (2005).
<https://doi.org/10.1016/B978-012464786-2/50010-9>
- [86] Nicolaou K. C., Snyder S. A., Montagnon T., Vassiliko-giannakis G.: The Diels-Alder reaction in total synthesis. *Angewandte Chemie – International Edition*, **41**, 1668–1698 (2002).
[https://doi.org/10.1002/1521-3773\(20020517\)41:10<1668::AID-ANIE1668>3.0.CO;2-Z](https://doi.org/10.1002/1521-3773(20020517)41:10<1668::AID-ANIE1668>3.0.CO;2-Z)
- [87] Karami Z., Zolghadr M., Zohuriaan-Mehr M. J.: Self-healing Diels–Alder engineered thermosets. in ‘Self-healing polymer-based systems’ (eds.: Thomas S., Surendran A.) Elsevier, Amsterdam, 209–233 (2020).
- [88] Brancart J., Verhelle R., Mangialetto J., van Assche G.: Coupling the microscopic healing behaviour of coatings to the thermoreversible Diels-Alder network formation. *Coatings*, **9**, 13 (2019).
<https://doi.org/10.3390/coatings9010013>